

# Design and Integration of Inkjet-printed Paper-Based UHF Components for RFID and Ubiquitous Sensing Applications

Amin Rida<sup>#1</sup>, Li Yang, Rushi Vyas, Swapan Bhattacharya, and Manos M. Tentzeris

<sup>#</sup>Georgia Electronic Design Center, School of Electrical and Computer Engineering,  
Georgia Institute of Technology, Atlanta, GA 30332-0250, USA

<sup>1</sup>arida@ece.gatech.edu

**Abstract**— Paper is one of the best substrate candidates for Radio Frequency Identification (RFID) and ubiquitous sensing applications due to the fact that it is not only one of the lowest cost materials, but is environmentally friendly and can be easily used for mass reel-to-reel processing. In this paper, the UHF/RF electrical characterization of the paper substrate, using the microstrip ring resonator method, has been performed yielding an accurate low-value range for the dielectric constant ( $\epsilon_r$ ) and loss tangent ( $\tan\delta$ ). A UHF RFID antenna is designed and inkjet printed on paper to demonstrate the applicability of this material. The presented approach could potentially set the foundation for very large ultra-low-cost ad-hoc networks for cognitive radio and sensing applications.

## I. INTRODUCTION

The demand for inexpensive, flexible, reliable, low-power consumption and durable wireless RFID-enabled sensor nodes is driven by several applications, such as logistics, Aero-ID, anti-counterfeiting, supply-chain monitoring, space, healthcare, pharmaceutical, and is regarded as one of the most important methods for realizing ubiquitous ad-hoc networks. Compared with the lower frequency tags operating in the LF and HF bands, that suffer from limited read range (up to 1 meter), RFID tags operating in the UHF band are forecast to find the widest use due to their higher read range (up to 9 meters in passive RFID configurations) and higher data transfer rate (currently 640 kbps for Gen 2 RFID standard).

Paper is considered as one of the best organic substrates to be used for RFID applications for several reasons. It is environmentally friendly, one of the cheapest materials known, can go large reel to reel processing, and has a low surface profile. This means that paper is an excellent substrate for mass production of RFID tags, and since it is compatible with circuit printing by direct write methodologies; fast conductive paste inkjet processes may further enhance its applicability. This also enables modules such as: antennas, IC, memory, batteries and/or sensors to be easily embedded in/on paper. In addition, paper can be made hydrophobic and/or fire-retardant by adding certain textiles.

In this paper, for the first time, the electrical characterization of dielectric constant ( $\epsilon_r$ ) and loss tangent ( $\tan\delta$ ) characterization[1,2] of paper over the frequency range 0.4 GHz to 2.4 GHz has been developed using the microstrip ring resonator method. First, one microstrip line was fabricated on photo paper for the measurement of  $\epsilon_r$  and  $\tan\delta$ .

An RFID tag module using series and shorting stubs for the matching of the antenna terminals to the Integrated Circuit (IC) was designed and printed on the characterized paper substrate using inkjet printing technology.

## II. CHARACTERIZATION OF PAPER SUBSTRATE USING MICROSTRIP RING RESONATOR METHOD

The two most important electrical parameters used to characterize an RF/microwave substrate are the dielectric constant and the loss tangent. Dielectric constant ( $\epsilon_r$ ) determines the characteristic impedance of circuitry, such as transmission lines width, and physical parameters of antennas and other passive components, such as microwave filters. Loss tangent ( $\tan\delta$ ) determines the amount of loss in the dielectric medium and hence determines if a substrate is appropriate for a certain application depending on its power level requirements.

In this paper, one microstrip resonator was designed and fabricated on a 700  $\mu\text{m}$  thick photo paper substrate. In order to achieve this thickness, 4 sheets of 263  $\mu\text{m}$  thick photo paper were pressed using the PHI laminator Q-247C4 for the bonding process with a 10 tons RAM force applied under 200 °F. 18  $\mu\text{m}$  copper sheets were laminated on each side of the substrate using the same bonding process discussed above. Wet etching process was utilized for the fabrication of the ring resonator and the through-reflect-lines (TRL) used for calibration. Compared with microstrip line resonators, a microstrip ring resonator does not suffer from open-ended effects [2] especially after performing TRL calibration. However;  $\tan\delta$  extractions using the microstrip ring resonator approach requires reliable theoretical equations for the estimation of the conductor losses.

The ring resonator produces  $S_{21}$  results with periodic frequency resonances. In this method,  $\epsilon_r$  can be extracted from the location of the resonances of a given radius ring resonator while  $\tan\delta$  is extracted from the quality factor (Q) of the resonance peaks along with the theoretical calculations of the conductor losses.

Simulations were performed using Ansoft HFSS full wave simulator and the measurements were done over the frequency range 0.4 GHz to 1.5 GHz using Agilent 8530A Vector Network Analyzer (VNA). Typical SMA coaxial connectors were used to feed the ring resonator structure. TRL calibration

was performed to de-embed the input and output microstrip feeding lines effects and eliminate any impedance mismatch. TRL lines consisted of 6 microstrip lines; 4 of which were  $\lambda/4$  long in addition to the input and output microstrip feeding lines at the frequencies: 0.75GHz, 1 GHz, 2GHz, and 3 GHz; the other 2 lines consisted of a Reflect-open and a through line which corresponded to the length of the input and output feeding lines added together. This method sets a reference plane to the edge of the gap such that only the microstrip ring resonator is effectively measured [3].

Fig. 1 shows a layout of the ring resonator along with the dimensions for the length of microstrip feeding lines, the gap in between the microstrip lines and the microstrip ring resonator, the width of the signal lines, and the mean radius  $r_m$ . The gap between the feeding lines and the ring is what causes the coupling into the ring resonator. Fig. 2 shows a photo of the fabricated ring with the TRL lines.

$S_{21}$  magnitude vs. frequency data were then inserted in a Mathcad program and the dielectric constant and loss tangent were extracted [1] [2]. A plot of  $S_{21}$  vs. frequency is shown in Fig. 3.

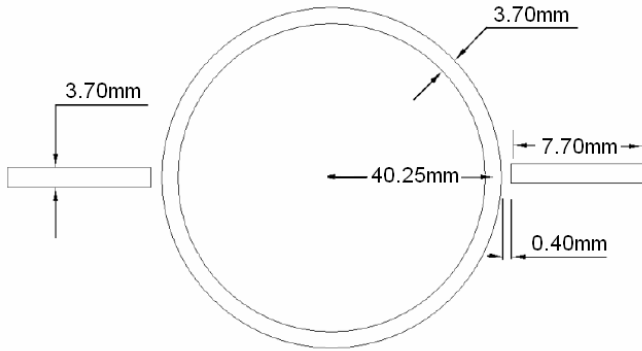


Fig. 1 Microstrip ring resonator configuration diagram.

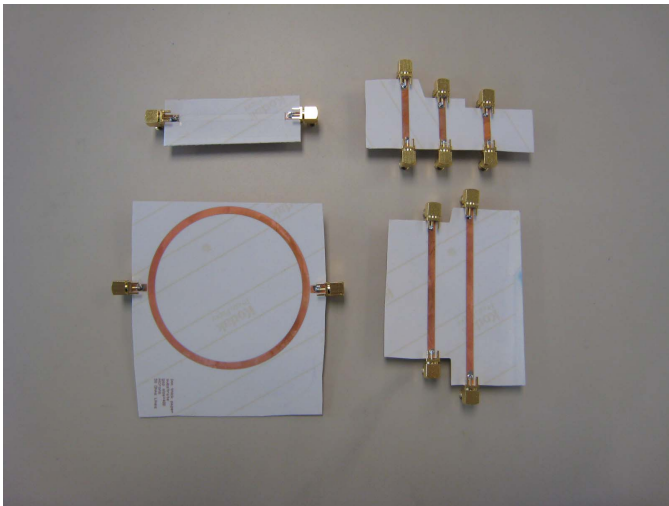


Fig. 2. Photo of fabricated Microstrip ring resonators and TRL lines.

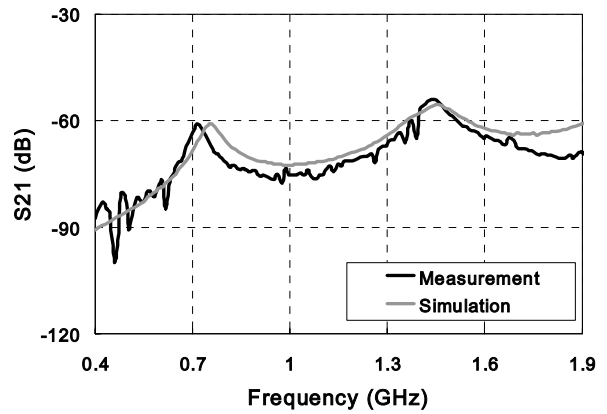


Fig. 3  $S_{21}$  vs. frequency for the resonator of Fig.1.

#### A. Dielectric constant

The desired resonant peaks were obtained according to [1]:

$$f_o = \frac{nc}{2\pi r_m \sqrt{\epsilon_{eff}}} \quad (1)$$

where  $f_o$  corresponds to the  $n$ th resonance frequency of the ring with a mean radius of  $r_m$  and effective dielectric constant  $\epsilon_{eff}$  with  $c$  being the speed of light in vacuum.

The extracted  $\epsilon_r$  value at the first, and second resonances (up to 1.5 GHz) of Fig. 3 were obtained using equation 1 and are shown in Table I.

#### B. Dielectric Loss

The extraction of loss tangent was performed after subtracting the theoretical values of conductor and radiation losses. This is required to isolate the dielectric loss  $\alpha_d$  since the ring resonator method gives the total loss at the frequency locations of the resonant peaks. The loss tangent is a function of  $\alpha_d$  (in Nepers/m) according to [1]:

$$\tan \delta = \frac{\alpha_d \alpha_o \sqrt{\epsilon_{eff}} (\epsilon_r - 1)}{\pi \epsilon_r (\epsilon_{eff} - 1)} \quad (2)$$

where  $\lambda_o$  is the free-space wavelength,  $\epsilon_r$  and  $\epsilon_{eff}$  are the same as described above.

Available theoretical methods for calculating conductor loss and radiation loss have been dated from the 1970s[1].  $\tan \delta$  results are shown in Table I for 2 modes (up to 1.5 GHz) after subtracting the calculated conductor and radiation losses.

TABLE I  
RESULTS OF RING RESONATOR DIELECTRIC EXTRACTION

Mode	Resonant Freq ( $f_0$ )	Insertion Loss ( $ S_{21} $ )	BW <sub>3dB</sub>	$\epsilon_r$	$\tan\delta$
n=1	0.71 GHz	-61.03 dB	42.12 MHz	3.28	0.061
n=2	1.44 GHz	-53.92 dB	75.47 MHz	3.20	0.053

### C. Results and Discussion

It is to be noted that the density of the paper substrate slightly increases after the bonding process described above. This may slightly increase the calculated dielectric constant in Table I for multilayer paper-based RF modules.

### III. INKJET PRINTED RFID ANTENNA ON PAPER SUBSTRATE

As a preliminary demonstration to an all-printed RFID module, a passive RFID tag was developed in this section. Despite the fact that passive RFID tags are in a tremendous demand due to their cost and fabrication advantages, their practical large-scale implementation is impeded by the challenge of their miniaturized implementation in the UHF RFID frequency range (866 MHz to 868 MHz in Europe and 902 MHz to 928 MHz in North America). Another challenge is the matching of passive RFID antennas to the impedance of the IC, which commonly exhibits complex (highly capacitive) impedance, for optimum power flow in/out of the passive tag while communicating with the reader.

The antenna developed in this section was simulated using the electrical parameters obtained in section II. The half-wavelength tapered-width U-shaped antenna is shown in Fig. 4. This antenna has been printed using inkjet printing technology using silver paste as the conductor. The two stubs, namely inductive and shorting stubs, shown in Fig. 4 are responsible for the matching of the antenna terminals to the IC impedance of value  $73-j113$  Ohms, which is expected to have a flat response over the UHF RFID frequency band. The tapered width of the two arms offers an increased bandwidth compared with most of the available passive RFID tags that exhibit about 1-2 % bandwidth only [4].

The dimensions of this antenna are: 7.6 cm x 5.5 cm.

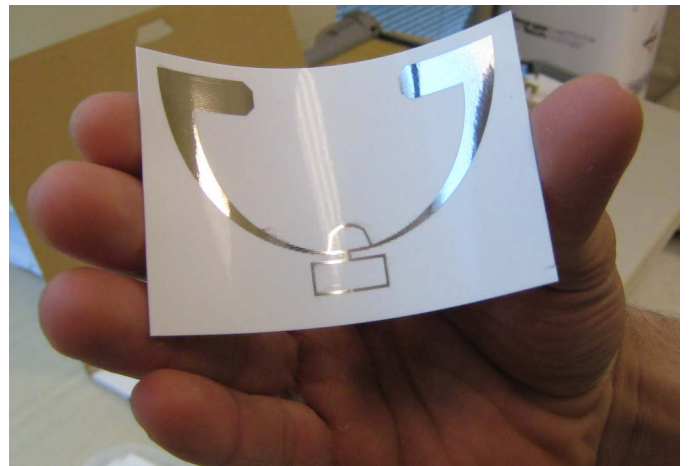


Fig. 4 Photograph of the inkjet printed U-shaped RFID passive antenna along with the integrated matching stubs

The Return Loss (RL) plot is shown in Fig. 5 below. The VSWR of 2 or RL of -9.6dB defines the bandwidth of operation. This antenna operates from 855 MHz to 887 MHz, centered around 872 MHz and hence covers the European RFID UHF frequency band.

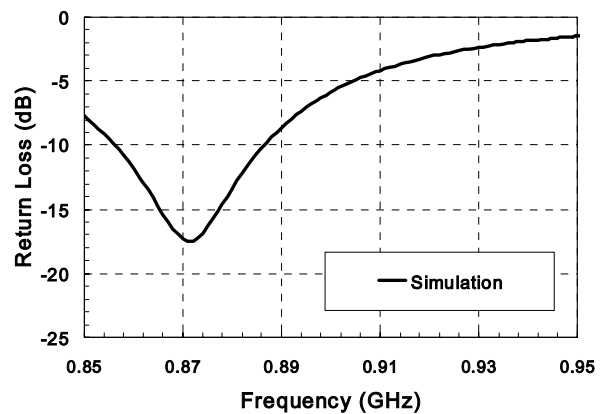


Fig. 5 Return loss simulations of the inkjet printed U-shaped RFID

Since this antenna belongs to the half-wavelength dipole family, it exhibits a uniform quasi-omnidirectional radiation pattern as shown in Fig. 6 below.

## V. CONCLUSIONS

The electrical properties of paper as a UHF substrate have been characterized using the microstrip resonator method. It was found that the dielectric constant in the UHF frequency is around 3.2 and loss tangent around 0.055 in the frequency range from 0.4 GHz to 1.5 GHz. An RFID passive module was designed and inkjet-printed on paper using the reported values of  $\epsilon_r$  and  $\tan\delta$  found, and verifies that paper can be an excellent substrate for ultra-low-cost single-layer/multilayer wireless nodes for telecom, sensing and security applications.

## REFERENCES

- [1] D. Thompson, G. Ponchak, M. M. Tentzeris, J. Papapolymerou, "Characterization of LCP material and transmission lines on LCP substrates from 30 to 110GHz," *IEEE Trans. Microwave Theory and Tech.*, vol. 52, no. 4, pp. 1343-1352, April 2004.
- [2] G. Zou, H. Gronqvist, J.P. Starski, and J. Liu, "Characterization of Liquid Crystal Polymer for High Frequency System-on-a-Package Applications," *IEEE Trans. Advanced Packaging*, vol. 25, no. 4, pp. 503-508, November 2002.
- [3] TRL Calibration Defined, online Article, available HTTP: <http://www.maurymicrowave.com/support/faqs/faqs/faq7.html>
- [4] "Design and Development of Novel Miniaturized UHF RFID Tags on Ultra-Low-Cost Paper-Based Substrates" L. Yang, S. Basat, A. Rida, and M. M. Tentzeris, APMC Dec 15, 2006.
- [5] S.Basat, S. Bhattacharya, L. Yang, A. Rida, M. M.Tentzeris, and J. Laskar, "Design of a Novel High efficiency UHF RFID Antenna on Flexible LCP Substrate with High Read-Range Capability," Proc. Of the 2006 IEEE-APS Symposium, pp.1031-1034, Albuquerque, NM, July 2006.
- [6] V. Subramanian, J. Frechet, "Progress toward development of all-printed RFID tags: materials, processes, and devices," *Proceedings of the IEEE*, vol. 93, no. 7, pp. 1330-1338, July 2005.

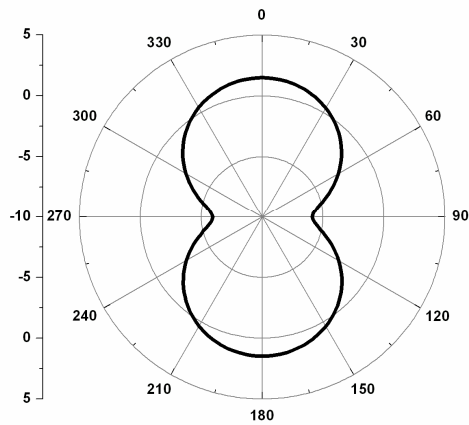


Fig. 6 Gain in dB of the inkjet printed U-shaped RFID at 866 MHz.

## IV. INTEGRATION OF IC, SENSORS, AND BATTERIES ON PAPER BASED RFID SUBSTRATES

In order to meet the ultra low cost demand for passive, semi-passive, and active RFID tags with increased (sensing, tracking, monitoring) functionality, the conductive ink printing technology on organic substrates, is suggested as an easy manufacturing approach. The ultimate goal is to have an all printed RFID tag (antenna, IC, battery, and sensor) on a low-cost environmentally friendly paper-based substrate.

Active tags, such as sensors and gel batteries [6] can also be printed on paper in a multilayer fashion. Paper substrate can handle high temperature treatment during the assembly process in an excellent way and the reliability/life time is very high compared to other substrates such as plastic. A suggested module of a printed UHF RFID active tag is shown in the figure below.

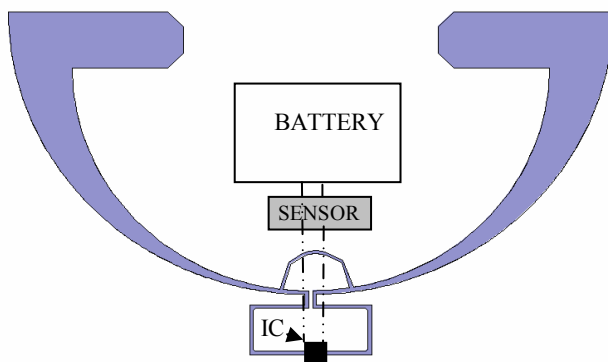


Fig. 7. Suggested outline of integrated U-shaped antenna with IC, sensor and embedded battery.